

Universal aspects of droplet spreading dynamics in Newtonian and non-Newtonian Fluids

B. Gorin,^{*,†,‡} G. Di Mauro,^{*,†} D. Bonn,^{*,†} and H. Kellay^{*,‡,¶}

[†]*Van der Waals Zeeman Institute, University of Amsterdam, 1018 XE Amsterdam, The Netherlands*

[‡]*Laboratoire Ondes et Matière d'Aquitaine, Université de Bordeaux, 33400 Talence, France*

[¶]*Institut Universitaire de France, 75005 Paris, France*

E-mail: benjamin.gorin@u-bordeaux.fr; gabrielle.di-mauro@espci.fr; D.Bonn@uva.nl;
hamid.kellay@u-bordeaux.fr

Abstract

Droplet impacts are common in many applications such as coating, spraying, or printing; understanding how droplets spread after impact is thus of utmost importance. Such impacts may occur with different velocities on a variety of substrates. The fluids may also be non-Newtonian and thus possess different rheological properties. How the different properties such as surface roughness and wettability, droplet viscosity and rheology as well as interfacial properties affect the spreading dynamics of the droplets and the eventual drop size after impact are unresolved questions.

Most recent work focuses on the maximum spreading diameter after impact and uses scaling laws to predict this. In this paper we show that a proper rescaling of the spreading dynamics with the maximum radius attained by the drop, and the impact velocity leads to a unique single and thus universal curve for the variation of diameter

versus time. The validity of this universal functional shape is validated for different liquids with different rheological properties as well as substrates with different wettabilities. This universal function agrees with a recent model that proposes a closed set of differential equations for the spreading dynamics of droplets.

Introduction

Droplet impacts are routinely studied¹ to understand a wide range of phenomena ranging from spraying, coating, printing²⁻⁵ to self cleaning and anti-icing.⁶ Typical examples abound from every day life or in industrial applications: a droplet of rain impacting a glass pane,⁷ the deposition of a molten metal droplet for electronic printing,⁸⁻¹⁰ or droplet impacts of polymers or surfactants solutions usually used for a more controlled deposition.¹¹⁻¹⁵ It is thus central to understand droplet spreading and give it a proper description. The difficulty of understanding droplet impacts stems from the fact that this process involves many different contributions such as viscous dissipation, surface tension effects, surface roughness, wetting and spreading as well as the dynamics of the contact line. It is therefore arduous to propose a simple description for the spreading dynamics upon impact and describe how the diameter of the drop $D(t)$ evolves with time t ¹⁶⁻²⁰. Many studies focus on the maximum spreading diameter D_{max} and propose different scaling laws using arguments of energy conservation²¹⁻²⁶. Recently, for the purpose of describing the dynamics of spreading of Newtonian fluids, a theory proposed by Gordillo et.al²⁷⁻²⁹ gives a solution for $D(t)$ by solving a system of equations describing the spreading of an impacting droplet. This model is based on modelling the spreading droplet as a thick rim followed by a thin liquid film connected to the bulk of the drop. Using mass and momentum conservation between the rim, the liquid film and the droplet, a set of coupled differential equations is proposed. Solving these equations with the proper boundary conditions leads to a complete description of $D(t)$ for Newtonian drops impacting a smooth surface. In this work, we carry out experiments of droplet spreading dynamics on a variety of fluids, with different rheological properties, impacting at different

velocities substrates with different wettabilities. Our results show that a simple rescaling of $D(t)$ with the maximum diameter D_{max} and a rescaling of the time scale by a characteristic time D_{max}/V_0 where V_0 is the impact velocity, leads to a single master curve describing the spreading dynamics of droplet impacts independently of the substrate, interfacial or rheological properties. Our scaling function agrees with the recent theory of Gordillo et.al²⁸. Our work therefore shows that the diameter $D(t)$ of spreading droplets depends only on the maximum spreading diameter D_{max} and the impact velocity V_0 .

Methods and materials

We perform a series of droplet impact experiments with different liquids (water, hexadecane, aqueous polymer solutions and Carbopol solutions) impacting different surfaces. The experimental setup is as follows: a syringe with a needle is fixed at a certain height which sets the impact velocity V_0 (varied between $1m.s^{-1}$ and $4m.s^{-1}$). The syringe is connected to a syringe pump to release droplets using very low injection fluxes. Droplet sizes D_0 can be varied between 1.80 and 4.5mm (all droplet diameters are given in the figure descriptions). The Reynolds and Weber numbers are defined as $Re = \frac{\rho V_0 D_0}{\eta}$ and $We = \frac{\rho V_0^2 D_0}{\sigma}$ where ρ , η and σ are respectively the density, the viscosity and the surface tension of the liquid. Different surfaces are used: smooth hydrophilic and hydrophobic microscope glass slides (hydrophobic coating with Octadecyltrichlorosilane) as well as parafilm. All experiments are done at room temperature $T = 23^\circ C$ and $RH = 40\%$. Droplet impacts are recorded at high framerates (up to 19000 fps) using a fast camera (Phantom V640) aligned with the substrate (see figure 1a,b and c).

The liquids used for the droplets are pure water, hexadecane and two types of non-Newtonian fluids. We use aqueous solutions of polymer (polyethylene oxide also called PEO) of molecular weight of $4.10^6 g.mol^{-1}$ at concentrations varying between 10 ppm and 5000 ppm. A small amount of isopropanol (about 1 wt %) is added to avoid polymer

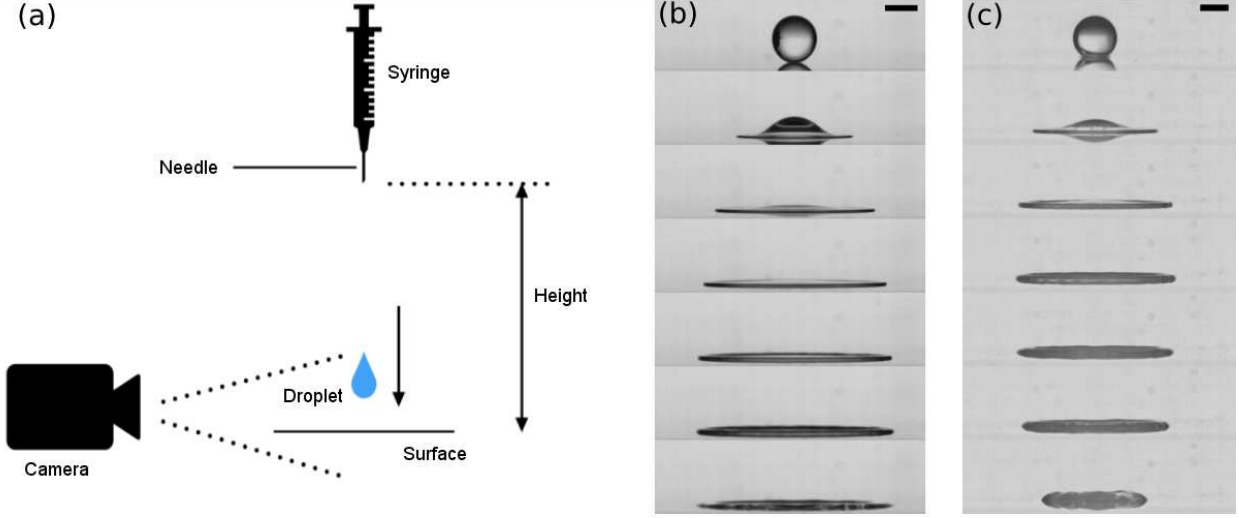


Figure 1: (a) experimental setup for measuring droplet impacts on a flat surface. (b) water droplet ($D_0 = 3.57 \text{ mm}$, $V_{0,a} = 2.29 \text{ m.s}^{-1}$, $Re = 8100$, $We = 260$) impacting a hydrophilic glass surface. (c) water droplet ($D_0 = 3.64 \text{ mm}$, $V_0 = 2.17 \text{ m.s}^{-1}$, $Re = 7900$, $We = 240$) impacting a hydrophobic glass surface. Snapshots are taken at 0-1-2-3-4-5-8 ms after impact. Scale bar : 2 mm

aggregation. Experiments are done using a yield stress fluid consisting of aqueous solutions of Carbopol at different concentrations. In all cases, we focus our study on drop impacts with high Reynolds numbers meaning that the spreading is mainly driven by droplet inertia. Further, drop impact velocities are chosen in such a way that splashing is avoided. The two Non-Newtonian fluids are used in order to test the role of the liquid rheology. The presence of polymer renders the viscosity of the liquid shear rate dependent and elastic polymer flow interactions can take place.^{30,31} Further experiments using Carbopol solutions are intended to examine how yield stress fluids affect the spreading^{32,33}.

The rheology of the polymer solutions (PEO) was measured using an Anton Paar rheometer with a cone plate geometry (two cones were used, angle 0.5° and diameter 60 mm and angle 1° and diameter 50 mm). For the Carbopol solutions the flow curves were measured using a rough cone-plate geometry (diameter = 40 mm , angle = $1^\circ 58'$, truncation gap = $59 \mu\text{m}$) on a controlled stress rheometer ARG2 (TA - Instruments). The relaxation time for the 5000 ppm PEO aqueous solutions using the Carreau Model is $\tau_r \sim 0.040 \text{ s}$. For Carbopol solutions, we use the same definition as proposed by Luu.et.al³⁴ to estimate a characteristic

time as : $\tau_r = (\frac{k}{G})^{1/n}$ where k is the fluid consistency (in $Pa.s^n$), G the elastic shear modulus (in $Pa.$) and n the flow index. The Deborah number is defined as the ratio of the relaxation

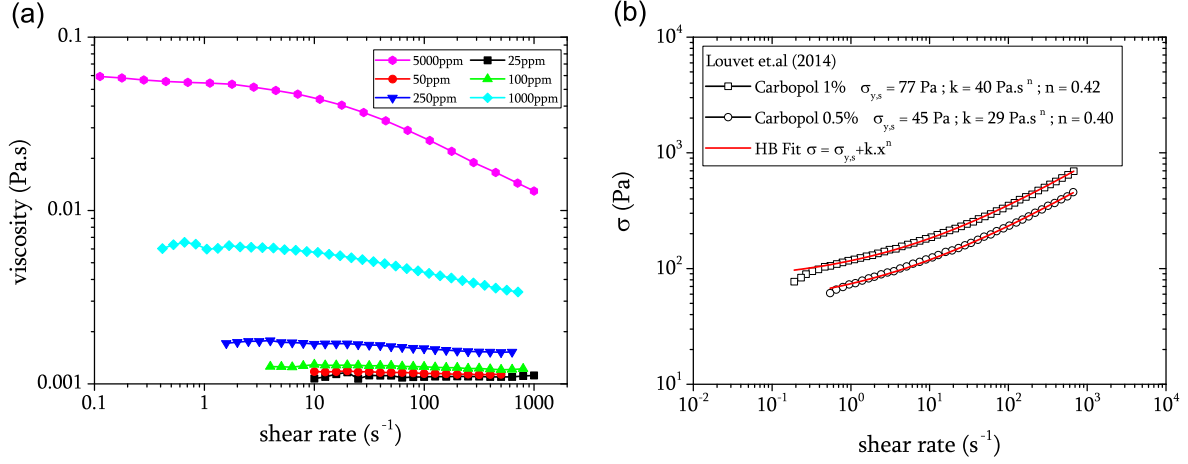


Figure 2: Rheology of (a) PEO at different concentrations and (b) Carbopol solutions at two different concentrations. The flow curves are fit to the Hershel Bulkley model $\sigma = \sigma_{ys} + kx^n$. Here x is the shear rate, n the flow index, k the consistency parameter, and σ_{ys} is the yield stress of the solution. The values of the parameters are given in the figure.

time τ_r deduced from the rheology of the system and the observation time $\tau = \frac{R_0}{V_0}$: $De = \frac{\tau_r}{\tau}$. For all impacts De was much greater than 1 (10 for the Carbopol solutions and 40 for the 5000ppm PEO solution at a velocity of 1m/s) so our drops behave like a fluid during the impact.

In general, when a droplet impacts a flat smooth surface, it follows three different regimes : An initial stage where the droplet spreads very quickly until it reaches a maximum spreading diameter D_{max} . In principle, during this stage, surface wettability is negligible compared to droplet inertia. When the droplet reaches its maximum spreading diameter, it enters a stage where wetting plays a role and the droplet can either retract or continue spreading³⁵ depending on the surface wettability.

In the work carried out here, most droplets retract because the impact velocity is sufficiently high that the maximum spreading diameter is always larger than the equilibrium spreading diameter $D_{max} > D_{eq}$. The retraction speed then depends on the wettability of the surface and the liquid properties.

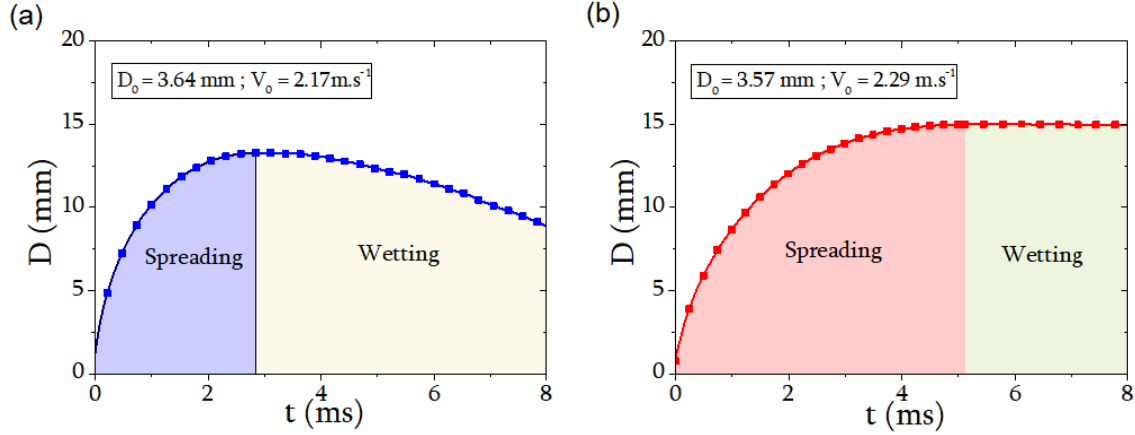


Figure 3: Spreading diameter dynamics $D(t)$ of a water drop of figure 1 impacting a (a) hydrophobic and (b) hydrophilic microscope glass slide

This phenomenology is illustrated in figure 3 where two experimental examples of the spreading dynamics $D(t)$ of droplets impacting different substrates are shown. In the first case little retraction is observed as the surface is hydrophilic. When the surface is highly hydrophobic, retraction occurs as in the second example. This retraction can lead to a possible rebound of the droplet. Here we only focus on the spreading dynamics until the droplets reach the maximum spreading diameter D_{max} .

Results and discussion

We first discuss the results for water drops impacting a hydrophilic and a hydrophobic glass substrate. This is shown in figures 4a and b. For both cases, the spreading is fast in the initial stages, reaches a maximum diameter, before settling on a quasi plateau value, figure 4a, or before retracting for the hydrophobic substrate, figure 4b. Note that the maximum spreading diameter as well as the speed of spreading increase as the velocity of impact increases as expected for both substrates. Our main result is shown in figure 4c. Here we replot the same data as figures 4a and 4b using rescaled variables. The time of evolution is rescaled as t/τ with $\tau = D_{max}/V_0$ while the diameter is rescaled as D/D_{max} . This figure

shows that the spreading diameter dynamics follows one single universal functional shape until it reaches its maximum value D_{max} with deviations occurring at later times. At these late times, either retraction occurs (in particular for the hydrophobic surface) or the droplet continues to spread slowly due to surface wettability. In these regimes, the collapse of the data ceases to apply.

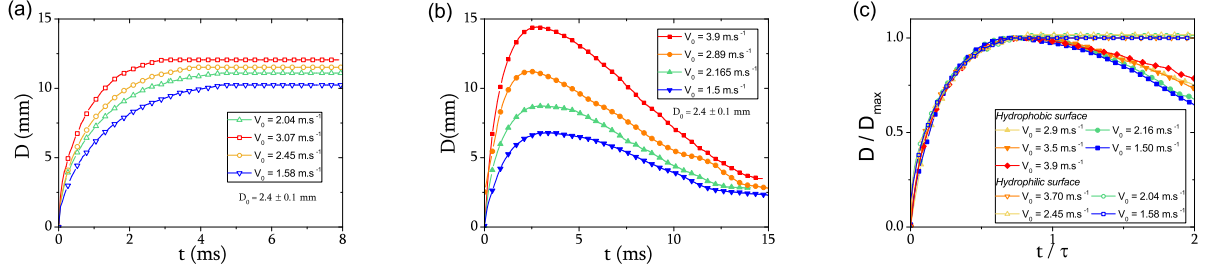


Figure 4: Spreading diameter dynamics of water droplets impacting two different substrates : (a) a hydrophilic glass and (b) a hydrophobic glass. (c) Rescaled spreading dynamic of water drop impacts. The Reynolds and Weber numbers varied between $3500 < Re < 8700$ and $77 < We < 470$

In fact this scaling function, for the spreading dynamics up to the moment where the maximum diameter is reached, is insensitive to the wettability of the substrate as the collapse of the data from the two substrates show. This is our main result and show that a proper rescaling of the diameter and the time scale collapses our data for different substrates, different initial diameters as well as different impact velocities. Does this rescaling persist for other fluids and rheological properties? This is what we examine next.

A surprising result comes from additional experiments carried out using polymer solutions. These solutions are non-Newtonian and show a shear thinning behaviour as shown in figure 2. The scaling function found for the case of pure water is not influenced by the presence of polymers despite the fact that such polymer solutions can present strong shear thinning behaviour and complex polymer flow interactions. This is illustrated in figure 5a for different polymer concentrations as well as different impact velocities. The spreading dynamics shows the usual features of increased maximum diameter and increased spreading speed versus impact velocity but also a retraction phase depending on the velocity and poly-

mer concentration¹². Figure 5b shows the rescaled data and the very good agreement with the scaling function for water. The spreading dynamics of Newtonian and non-Newtonian fluids can be described by the same universal spreading curve.

Besides the use of polymer solutions, we have carried out experiments using Carbopol solutions of different concentrations. The purpose of these experiments is to explore the role of the presence of a yield stress on the spreading dynamics. Our results are shown in Figure 6a. In all experiments, the inertial pressure defined as ρV_0^2 which is of order 10^3 or greater is systematically greater than the yield stress which is of order 10. Again, a proper rescaling of the data shows the presence of a universal collapse (see figure 6b) of the dynamics of the spreading up to D_{max} for different impact velocities and different concentrations and in excellent agreement with the functional form for the spreading of water droplets.

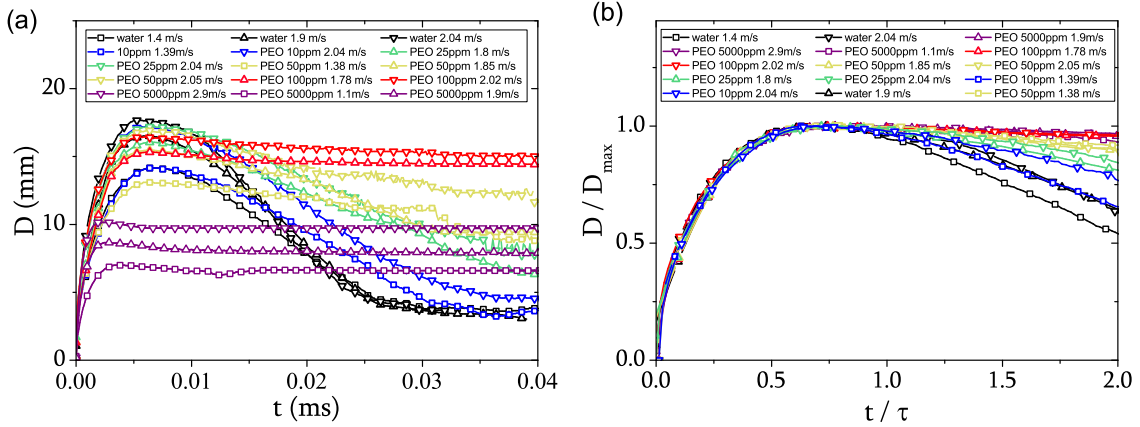


Figure 5: (a) Spreading dynamics of droplets of aqueous polymer solutions (PEO) at different concentrations and impact velocities. Water and PEO aqueous solutions at 10ppm, 25ppm, 50ppm and 100ppm are drop impacts on hydrophobic parafilm surfaces with a drop size of $D_0 = 4 \text{ mm}$ ($5200 < Re < 8000$ and $94 < We < 222$). Drop size of PEO 5000ppm is $D_0 = 3 \text{ mm}$ and spreads on hydrophobic glass ($150 < Re < 450$ and $41 < We < 375$). The viscosity used is taken at shear rates given close to V_0/D_0 (b) Rescaled spreading dynamics for all the droplets in a).

All the data obtained here follow the same scaling law and we show in figure 7, data from water, polymer solutions and Carbopol solutions rescaled by D_{max} and $\tau = D_{max}/V_0$. An excellent collapse of all of our data from different fluids and substrates emerges showing

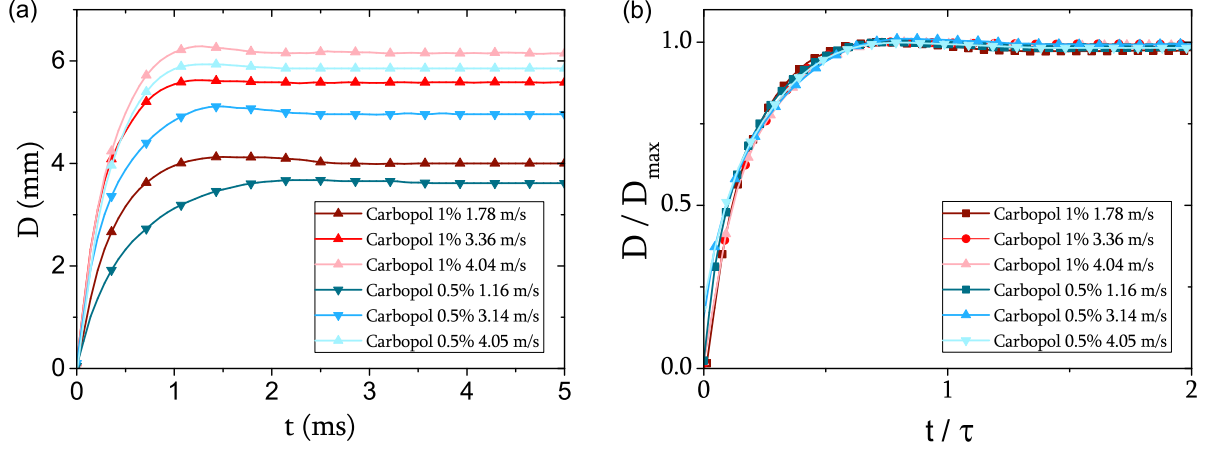


Figure 6: (a) Spreading dynamics of drop impacts of gel solutions made of water and Carbopol with two different concentrations (0.5% and 1%). Drop size is $D_0 = 2.3\text{mm}$ and surface used is a hydrophilic microscope glass ($46 < We < 736$ and $5 < Re < 31$ and $3 < De < 12$). The viscosity used is taken at shear rates given close to V_0/D_0 while the surface tension used is that of water. (b) Rescaled spreading dynamics for all droplets in a).

that the dynamics of spreading, independently of rheology and substrate properties, follows a universal functional form when rescaled properly.

The rescaling of the data as proposed here shows that the spreading phase of impacting droplets follows a simple scaling function $\frac{D(t)}{D_{max}} = f(t/\tau)$. This function depends only on D_{max} and V_0 . We find that this scaling function is in excellent agreement with the solution proposed by Gordillo et.al.²⁸ Indeed, the proposed solution $D(t)$ can be found by solving a system of equations using Matlab ODE45 solver :

$$\alpha \frac{\pi db^2}{4} \frac{dv}{dt} = [u(s, t) - v]h(s, t) \quad (1)$$

$$\alpha \frac{\pi b^2}{4} \frac{dv}{dt} = [u(s, t) - v]^2 h(s, t) - (1 + \beta)We^{-1} \quad (2)$$

$b(t)$ is the thickness of the rim, $s(t)$ the spreading diameter, $h(s, t)$ and $u(s, t)$ are respectively the thickness and the average velocity of the thin film between the droplet and the rim, $v = \frac{ds}{dt}$ the spreading velocity of the rim and α and β are two constants which are defined by the hydrophobicity of the substrate and the dynamic contact angle respectively. $\alpha = 1$ when

substrate is hydrophobic so the rim is lifted and thus considered with a circular shape and $\alpha = 1/2$ in case of hydrophilic surface. In our case, $\alpha = 1/2$ and $\beta = 0$. The results of this model are shown in figure 7

We have solved the system of equations proposed and rescaled the solution of the coupled equations in the same way as the experiments. The agreement between the theory of Gordillo et.al²⁸, and our results shown in figure 7 is excellent.

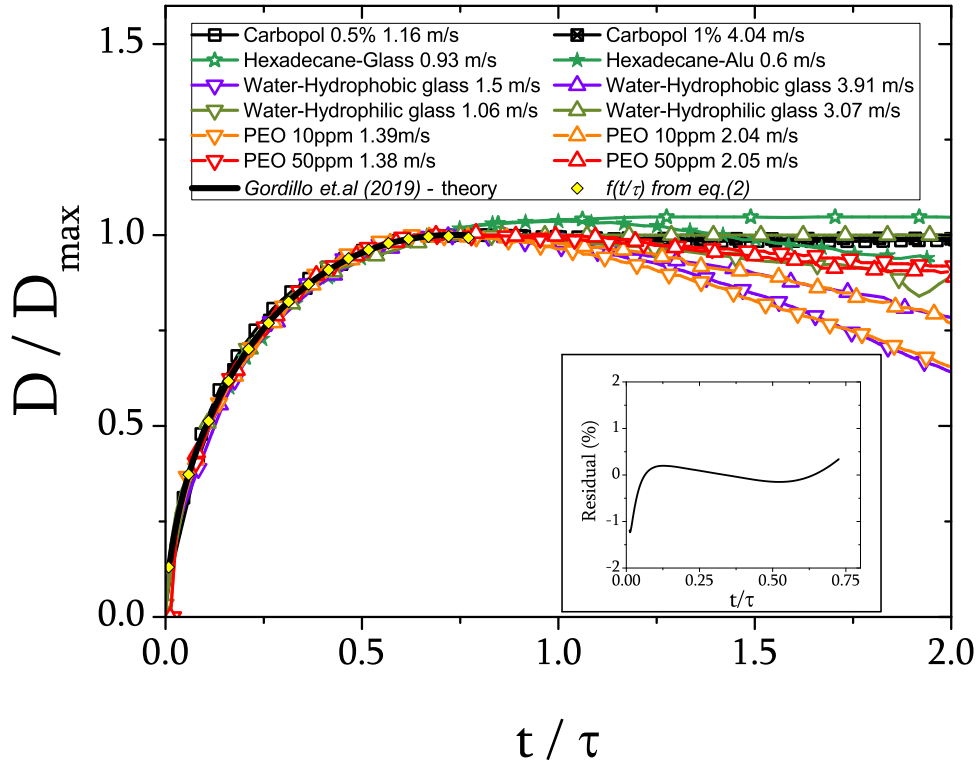


Figure 7: Rescaled spreading diameter of droplet impacts using different liquids, surfaces, drop size or impact velocities. Surface and droplet size D_0 used for each curves are the follow : Carbopol with hydrophilic glass and $D_0 = 2.28mm$. Hexadecane with hydrophilic glass and $D_0 = 1.90mm$. Water with hydrophilic and hydrophobic glass and $D_0 = 2.04mm$. PEO with hydrophobic parafilm and $D_0 = 4.0mm$. The inset shows the difference between the polynomial fit and the full Gordillo solution.

This master curve can be used to predict the spreading dynamics of any droplet impact. While the impact velocity is a known parameter, the maximum spreading diameter D_{\max} needs to be found or measured. Simple expressions for D_{\max} such as the one proposed by

Laan et.al^{24,25} can be used to find this value. This expression relates the maximum diameter to the Weber and Reynolds numbers of the droplet defined by $Re = \frac{\rho V_0 L}{\eta}$ and $We = \frac{\rho V_0^2 L}{\gamma}$ and is given by the following relation :

$$\frac{D_{max}}{D_0} = \frac{\sqrt{P}}{A + \sqrt{P}} Re^{1/5} \quad (3)$$

with the impact number $P = We Re^{-2/5}$ and a fitting constant $A = 1.24$.

Once the impact velocity and maximum diameter are known, our scaling function can then be used to deduce the diameter at any instant of time. For convenience and ease of use $f(t/\tau)$ can be approximated reliably by a simple a polynomial function of the form :

$$f(t/\tau) = a(t/\tau)^{1/2} + b(t/\tau) + c(t/\tau)^{3/2} \quad (4)$$

The constants a , b and c take the values : $a = 1.401 \pm 0.002$, $b = 0.903 \pm 0.008$, $c = -1.379 \pm 0.007$. This functional form starts out as $t^{1/2}$ at early times in accord with previous observations^{16,19} with corrections at later time in powers of $t^{1/2}$. The difference between this polynomial fit and the full solution is shown in the inset of figure 7 where a deviation of less than a percent is observed.

The rescaling we propose as well as the agreement found with the Gordillo model has, necessarily, some limitations. Rescaling works only for drop impacts at sufficiently high velocities for which the effects of surface wettability can be neglected compared to inertia. We actually kept impact velocities sufficiently high so that droplets spread engendering a liquid film with a rim at its edge in most cases as required in the theory of Gordillo et.al. For the non Newtonian cases, the Deborah number and the impact velocities were kept large enough so that the drops can be considered as fluid by assuring that the Deborah number is much greater than 1 and that the inertial pressure is systematically larger than the yield stress. Despite these limitations, the rescaling works remarkably well up to droplet the maximum spreading of the droplets. Further, we anticipate that the proposed rescaling

could be useful in other cases. Droplets impacting superheated surfaces leading to Leidenfrost drop impacts^{36,37} or droplets impacting super-hydrophobic substrates were not studied, but it is possible that the proposed rescaling may also be useful in such exotic cases.

Conclusion

We have provided a simple method to predict the spreading diameter $D(t)$ of a droplet impacting a flat surface. Spreading dynamics can be described by a universal curve for droplet impacts of Newtonian and non Newtonian fluids. This master curve is in addition in excellent agreement with the results of a theoretical model proposed recently Gordillo et.al²⁸. A closed functional shape is suggested in the form of a polynomial function to approximate the spreading dynamics for any impact velocity, droplet size, different substrates and fluid types.

References

- (1) Josserand, C.; Thoroddsen, S. Drop Impact on a Solid Surface. *Annual Review of Fluid Mechanics* **2016**, *48*, 365–391, _eprint: <https://doi.org/10.1146/annurev-fluid-122414-034401>.
- (2) Hoath, S. D. *Fundamentals of inkjet printing: the science of inkjet and droplets*; John Wiley & Sons, 2016.
- (3) Glasser, A.; Cloutet, E.; Hadziioannou, G.; Kellay, H. Tuning the Rheology of Conducting Polymer Inks for Various Deposition Processes. *Chemistry of Materials* **2019**, *31*, 6936–6944, Publisher: American Chemical Society.
- (4) Xie, K.; Glasser, A.; Shinde, S.; Zhang, Z.; Rampnoux, J.-M.; Maali, A.; Cloutet, E.; Hadziioannou, G.; Kellay, H. Delamination and Wrinkling of Flexible Conductive

- Polymer Thin Films. *Advanced Functional Materials* **2021**, *31*, 2009039, _eprint: <https://onlinelibrary.wiley.com/doi/pdf/10.1002/adfm.202009039>.
- (5) Lohse, D. Fundamental Fluid Dynamics Challenges in Inkjet Printing. *Annual Review of Fluid Mechanics* **2022**, *54*, 349–382, _eprint: <https://doi.org/10.1146/annurev-fluid-022321-114001>.
 - (6) Thiévenaz, V.; Séon, T.; Josserand, C. Solidification dynamics of an impacted drop. *Journal of Fluid Mechanics* **2019**, *874*, 756–773.
 - (7) Cebeci, T.; Kafyeke, F. AIRCRAFT ICING. *Annual Review of Fluid Mechanics* **2003**, *35*, 11–21, _eprint: <https://doi.org/10.1146/annurev.fluid.35.101101.161217>.
 - (8) Fukanuma, H. A porosity formation and flattening model of an impinging molten particle in thermal spray coatings. *Journal of Thermal Spray Technology* **1994**, *3*, 33–44.
 - (9) Tavakoli, F.; Davis, S. H.; Kavehpour, H. P. Spreading and Arrest of a Molten Liquid on Cold Substrates. *Langmuir* **2014**, *30*, 10151–10155, Publisher: American Chemical Society.
 - (10) Gielen, M. V.; Ruiter, R. d.; Koldeweij, R. B. J.; Lohse, D.; Snoeijer, J. H.; Gelderblom, H. Solidification of liquid metal drops during impact. *Journal of Fluid Mechanics* **2020**, *883*, A32.
 - (11) Bergeron, V.; Bonn, D.; Martin, J. Y.; Vovelle, L. Controlling droplet deposition with polymer additives. *Nature* **2000**, *405*, 772–775, Nature Research Journals Number: 6788 Publisher: Nature Publishing Group.
 - (12) Bartolo, D.; Josserand, C.; Bonn, D. Retraction dynamics of aqueous drops upon impact on non-wetting surfaces. *Journal of Fluid Mechanics* **2005**, *545*, 329–338, Publisher: Cambridge University Press.

- (13) Bartolo, D.; Boudaoud, A.; Narcy, G.; Bonn, D. Dynamics of Non-Newtonian Droplets. *Physical Review Letters* **2007**, *99*, 174502, Publisher: American Physical Society.
- (14) Jalaal, M.; Seyfert, C.; Stoeber, B.; Balmforth, N. J. Gel-controlled droplet spreading. *Journal of Fluid Mechanics* **2018**, *837*, 115–128, Publisher: Cambridge University Press.
- (15) Hoffman, H.; Sijs, R.; de Goede, T.; Bonn, D. Controlling droplet deposition with surfactants. *Physical Review Fluids* **2021**, *6*, 033601.
- (16) Biance, A.-L.; Clanet, C.; Quéré, D. First steps in the spreading of a liquid droplet. *Physical Review E* **2004**, *69*, 016301, Publisher: American Physical Society.
- (17) Eggers, J.; Fontelos, M. A.; Josserand, C.; Zaleski, S. Drop dynamics after impact on a solid wall: Theory and simulations. *Physics of Fluids* **2010**, *22*, 062101, Publisher: American Institute of Physics.
- (18) Lagubeau, G.; Fontelos, M. A.; Josserand, C.; Maurel, A.; Pagneux, V.; Petitjeans, P. Spreading dynamics of drop impacts. *Journal of Fluid Mechanics* **2012**, *713*, 50–60, Publisher: Cambridge University Press.
- (19) Eddi, A.; Winkels, K. G.; Snoeijer, J. H. Short time dynamics of viscous drop spreading. *Physics of Fluids* **2013**, *25*, 013102, arXiv: 1209.6150.
- (20) Wildeman, S.; Visser, C. W.; Sun, C.; Lohse, D. On the spreading of impacting drops. *Journal of Fluid Mechanics* **2016**, *805*, 636–655, Publisher: Cambridge University Press.
- (21) Madejski, J. Droplets on impact with a solid surface. *International Journal of Heat and Mass Transfer* **1983**, *26*, 1095–1098.
- (22) Clanet, C.; Béguin, C.; Richard, D.; Quéré, D. Maximal deformation of an impacting

- drop. *Journal of Fluid Mechanics* **2004**, *517*, 199–208, Publisher: Cambridge University Press.
- (23) Ukiwe, C.; Kwok, D. Y. On the Maximum Spreading Diameter of Impacting Droplets on Well-Prepared Solid Surfaces. *Langmuir* **2005**, *21*, 666–673.
 - (24) Laan, N.; de Bruin, K. G.; Bartolo, D.; Josserand, C.; Bonn, D. Maximum Diameter of Impacting Liquid Droplets. *Physical Review Applied* **2014**, *2*, 044018.
 - (25) Lee, J. B.; Derome, D.; Guyer, R.; Carmeliet, J. Modeling the Maximum Spreading of Liquid Droplets Impacting Wetting and Nonwetting Surfaces. *Langmuir* **2016**, *32*, 1299–1308.
 - (26) Wei, Y.; Thoraval, M.-J. Maximum spreading of an impacting air-in-liquid compound drop. *Physics of Fluids* **2021**, *33*, 061703, Publisher: American Institute of Physics.
 - (27) Riboux, G.; Gordillo, J. M. Maximum drop radius and critical Weber number for splashing in the dynamical Leidenfrost regime. *Journal of Fluid Mechanics* **2016**, *803*, 516–527, Publisher: Cambridge University Press.
 - (28) Gordillo, J. M.; Riboux, G.; Quintero, E. S. A theory on the spreading of impacting droplets. *Journal of Fluid Mechanics* **2019**, *866*, 298–315, Publisher: Cambridge University Press.
 - (29) García-Geijo, P.; Quintero, E. S.; Riboux, G.; Gordillo, J. M. Spreading and splashing of drops impacting rough substrates. *Journal of Fluid Mechanics* **2021**, *917*, Publisher: Cambridge University Press.
 - (30) Ingremau, F.; Kellay, H. Stretching Polymers in Droplet-Pinch-Off Experiments. *Physical Review X* **2013**, *3*, 041002, Publisher: American Physical Society.
 - (31) Bonn, D.; Meunier, J. Viscoelastic Free-Boundary Problems: Non-Newtonian Viscosity

- vs Normal Stress Effects. *Physical Review Letters* **1997**, *79*, 2662–2665, Publisher: American Physical Society.
- (32) Louvet, N.; Bonn, D.; Kellay, H. Nonuniversality in the Pinch-Off of Yield Stress Fluids: Role of Nonlocal Rheology. *Physical Review Letters* **2014**, *113*, 218302, Publisher: American Physical Society.
- (33) Martouzet, G.; Jørgensen, L.; Pelet, Y.; Biance, A.-L.; Barentin, C. Dynamic arrest during the spreading of a yield stress fluid drop. *Physical Review Fluids* **2021**, *6*, 044006, Publisher: American Physical Society.
- (34) Luu, L.-H.; Forterre, Y. Drop impact of yield-stress fluids. *Journal of Fluid Mechanics* **2009**, *632*, 301–327, Publisher: Cambridge University Press.
- (35) Tanner, L. H. The spreading of silicone oil drops on horizontal surfaces. *Journal of Physics D: Applied Physics* **1979**, *12*, 1473, Publisher: IOP Publishing.
- (36) Tran, T.; Staat, H. J. J.; Prosperetti, A.; Sun, C.; Lohse, D. Drop Impact on Superheated Surfaces. *Physical Review Letters* **2012**, *108*, 036101, Publisher: American Physical Society.
- (37) Staat, H. J. J.; Tran, T.; Geerdink, B.; Riboux, G.; Sun, C.; Gordillo, J. M.; Lohse, D. Phase diagram for droplet impact on superheated surfaces. *Journal of Fluid Mechanics* **2015**, *779*, Publisher: Cambridge University Press.

This figure "TOC_graphic.png" is available in "png" format from:

<http://arxiv.org/ps/2202.03109v1>